doi:10.1017/S1431927621001082
Microsc. Microanal. 27 (Suppl 1), 2021

Revealing Abnormal Phonon Polaritons Confined at the Edge of Curved Two-Dimensional Boron Nitride

Xingxu Yan[1], Jie Li[2], Lei Gu[2], Chaitanya Gadre[3], Samuel Moore[4], Toshihiro Aoki[5], Dmitri Basov[4], Ruqian Wu[6] and Xiaoqing Pan[3]

[1]Department of Materials Science and Engineering, University of California - Irvine, Irvine, California, United States, [2]Department of Physics and Astronomy, University of California - Irvine, Irvine, California, United States, [3]Department of Physics and Astronomy, University of California, Irvine, CA 92697, Irvine, California, United States, [4]Department of Physics, Columbia University, New York, New York, United States, [5]Irvine Materials Research Institute, University of California, Irvine, Irvine, California, United States, [6]Department of Physics and Astronomy, University of California, Irvine, CA 92697, United States

The hyperbolic phonon polariton (HPhP) is an emerging physical concept linked to many intriguing phenomena and has been explored in artificial metamaterial structures and a few single-phase natural materials [1]. Owing to its anisotropic dielectric function, two-dimensional (2D) hexagonal boron nitride (*h*-BN) can generate tunable HPhPs with low loss and long propagation length in different Reststrahlen bands [2]. However, the study of 1D propagating HPhPs, which are more promising for integrated optical circuits, is still absent in the *h*-BN nanostructures. Using monochromated electron energy-loss spectroscopy (EELS) in the scanning transmission electron microscope (STEM), we observe an abnormal HPhPs confined to within about 10 nm at the edge of folded *h*-BN flakes, which undergo an energy blue-shift up to 1.4 meV. Thanks to the atomic resolution capability of aberration-corrected STEM (AC-STEM), our approach can reveal nanoscale features of this confined HPhPs, which is inaccessible to optical methods due to their spatial resolution limitation.

Fig. 1b presents spatially resolved vibrational spectra across the edge of a folded 1L *h*-BN (Fig. 1a) acquired by monochromated Nion UltraSTEM 200 with an EELS energy resolution of ~7 meV at 60 keV. A single prominent peak occurs in all spectra, matching reported HPhP features recorded by EELS [3]. In the line profile of the peak center (Fig. 1d), there are three distinct regions. In the interior region away from the folding edge, the peak center is about 170 meV and remains unchanged. Meanwhile, we calculated the energy position of the HPhP in the *h*-BN slabs with different thickness [3, 4]. The calculated peak centers of 1L and 2L are 169.95 meV and 170.04 meV as indicated by two dashed lines in Fig. 1d. Thus, the HPhP signal in folded region can be assigned to the regular HPhP mode of 2L as a result of doubling the thickness of monolayer flakes. In the vacuum region (aloof configuration), a weak signal around 169 meV is observable and is consistent with the occurrence of hyperbolic surface phonon polaritons (HSPhPs) at the boundary of *h*-BN flakes [4, 5]. Strikingly, an energy blue-shifts takes place in HPhPs near the edge with an average increment of 1.4 meV compared to the interior folded region. Such an energy enhancement persists within ~10 nm near the edge.

To unearth the origin of the new edge-type HPhPs, we explored the influences of atomic alignment and sample thickness. By folding the *h*-BN flakes along different orientations, the local atomic structure at the curled edge is varied and depends on the twisting angle (TA) between top and bottom flakes. Figs. 2a and 2b display two representative low-voltage AC-STEM images of folded 1L and 2L *h*-BN with a Moiré pattern formed at the folded region. TA values can be determined by corresponding diffractograms, and the layer number is identified by counting the number of creases as marked in Fig. 2b. We conducted vibrational spectroscopy to track the energy offset of HPhPs from a variety of folding edges with various

TAs and layer numbers (1–3L) and summarized the results in Fig. 2c. The edge-type energy enhancements occur at all measured edges. Statistically, there seem to be an irregular fluctuation of the energy difference as a function of TA, which may arise from the sensitivity of the atomic alignment on the chirality. The folded bilayer samples exhibit the largest energy enhancement. Furthermore, first-principles calculations point out that the edge-type HPhPs originate from the local enhancement of dielectric functions, which can modify the dispersion curve of HPhPs. We can generate and manipulate the edge-type HPhPs by a top-down synthesis approach of electron-beam etching twisted *h*-BN bilayers. Our work opens an avenue of tailoring the local dielectric response and associated HPhP modes by folding few-layer *h*-BN flakes for applications in mid-infrared range devices [6].

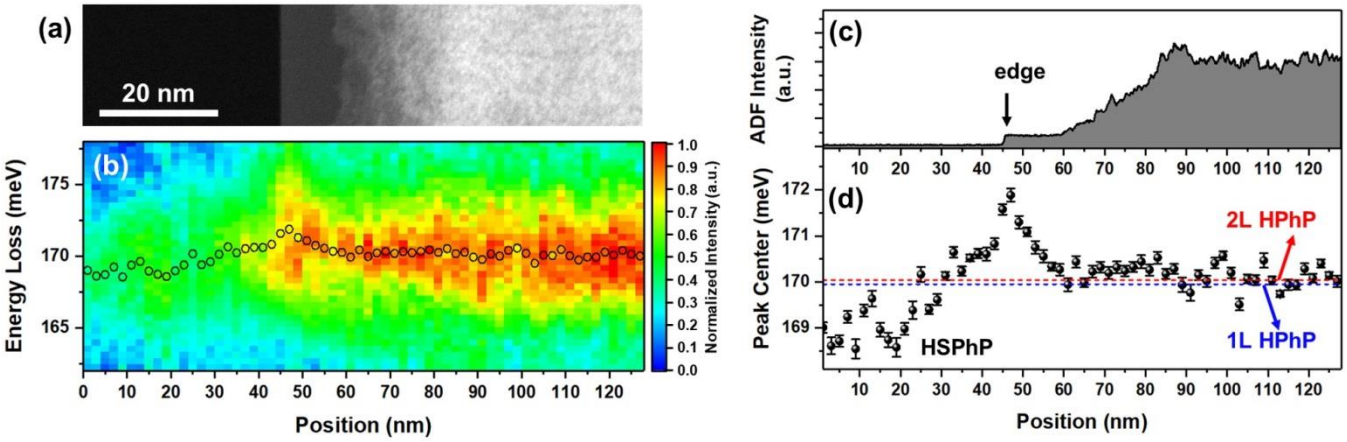

Figure 1. Figure 1. Vibrational spectra of confined HPhP signal in the folded 1L h-BN. (a) ADF-STEM image of an edge of freestanding folded 1L h-BN. Scale bar: 20 nm. (b) Line-scan of vibrational spectra from the same region in (a). The peak centers of HPhP signal are indicated as open dots. Color scale shows the spectral signal intensity normalized by its maximum value. (c) Line profile of ADF-STEM intensity in (a). (d) Line profile of peak center of HPhP in (b). Error bars represent the fitting error. Blue and red dashed horizontal lines represent the location of regular HPhPs in 1L and 2L h-BN, respectively.

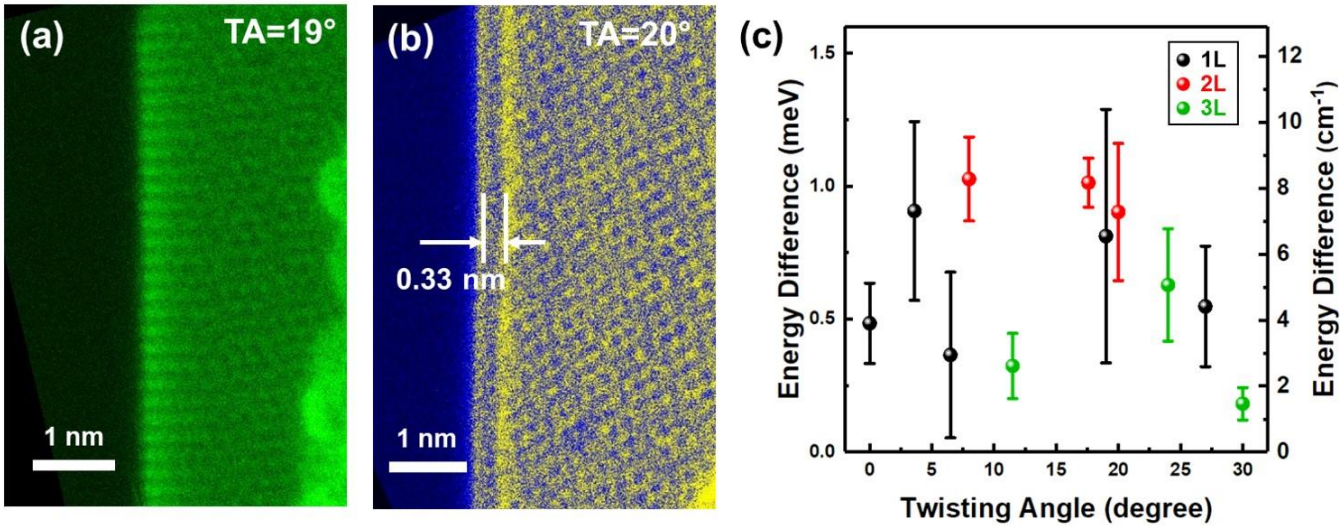

Figure 2. Figure 2. Influence of twisting angle and layer number on the edge-type HPhPs. (a) Atomic resolution STEM image of folded 1L h-BN with TA = 19°. (b) Atomic resolution STEM image of folded 2L h-BN with TA = 20°. The marked double crease with a separation of 0.33 nm confirms the folded bilayer

https://doi.org/10.1017/S1431927621001082 Published online by Cambridge University Press

structure. Scale bars in (a) and (b) are 1 nm. (c) The energy difference between the edge-type HPhPs and the one in the folded region against the twisting angle. Error bars represent the standard deviation.

References

[1] Z. Jacob, Nat. Mater. **13**, (2014), p. 1081–1083.

[2] S. Dai *et al.*, Science **343**, (2014), p. 1125–1129.

[3] A. A. Govyadinov *et al.*, Nat. Commun. **8** (2017), 95.

[4] N. Li, *et al.*, Nat. Mater. **20**, (2021), p. 43–48.

[5] S. Dai *et al.*, Adv. Mater. **30**, (2018), 1706358.

[6] This work was supported by the Department of Energy, Office of Basic Energy Sciences, Division of Materials Sciences and Engineering (DE-SC0014430). The authors acknowledge the use of facilities and instrumentation at the UC Irvine Materials Research Institute (IMRI) supported in part by the National Science Foundation through the Materials Research Science and Engineering Center program (DMR-2011967).